Trans. of the Society of Instrument and Control Engineers
Vol.E-2, No.1, 98/107 (2002)

Cascade Control Using GPC and LQR for a NO_x Reduction Process of a Thermal Power Plant

Masashi Nakamoto*, Takashi Kokubo**, Akinori Kamito* and Keiko Shimizu*

A control system for a selective catalytic nitrogen oxide (NO_x) reduction (SCR) process in a thermal power plant is developed using a Generalized Predictive Control (GPC) method and a Linear Quadratic Regulator (LQR) method. NO_x in gas turbine exhaust gas flow is decomposed by ammonia (NH_3) at catalysts. NH_3 flow rate is adjusted to keep the NO_x flow rate to a setpoint. The control system has a cascade scheme that includes NO_x control designed by a GPC method and NH_3 control designed by an LQR method. Experimental results on an actual plant during commercial operations show not only control performance but also practicability.

Key Words: GPC, LQR, Thermal Power Plant, DeNOx

1. Introduction

This paper describes a selective catalytic NO_x reduction (SCR) control system using a Generalized Predictive Control (GPC) and a Linear Quadratic Regulator (LQR) and presents test results on a commercial power plant which show not only its performance but also its usefulness.

In a thermal power plant, an SCR process facilitates to reduce NO_x emission [8], where NO_x gas is decomposed by NH_3 gas. The NO_x flow is generated by combustion of fossil fuel and its flow rate changes frequently according to the change of the plant operation. The purpose of the SCR control system is to keep the NO_x emission rate to the setpoint by adjusting the the NH_3 flow rate.

Thermal power plants change the operation frequently, which include start up and shut down, in order to adjust the electricity to the demand from a power system. Therefore, it is required for an SCR process control that has a good performance for a disturbance rejection and robustness. And it is also preferable not to need large memory and computational load in an economical point of view.

The SCR control has a cascade scheme and consists of the NO_x control and the NH_3 control. The NO_x control sets a reference of an NH_3 flow rate in order to keep the NO_x emission rate to the NO_x setpoint. The NH_3 control adjusts the NH_3 flow rate to the setpoint given by the NO_x control and retains the NH_3 pressure within allowable range. The NO_x control system has a large dead time that is caused by a gas analyzing system. The NH_3 process is an interactive multivariable system with two inputs and two outputs.

Conventionally the SCR process control is configured by proportional and integral (PI) controllers with a disturbance feedforward. Since a PI controller is not effective for systems with large dead times, a feedforward control works primarily. It is often required a complex calculation to obtain an adequate feedforward signal to take into account a various operation of a thermal power plant. In order to improve the control performance, there have been many trials which include a real time optimization with a nonlinear SCR model [5] and a Fuzzy logic control [4),13]. These methods require exact process models or complex tuning rules.

An SCR control system which includes a GPC and a feedforward control is reported [11]. As these controllers have been designed independently, there happen unpreferable responses at the disturbance change.

A multivariable control design is effective for a process which has an interaction such as an NH_3 control. Although some practical applications are reported [12], it is still not popular for a control of a power plant.

The feedback performances and the disturbance rejection of the NO_x control are improved by using GPC which takes into account the feedforward control. The performance of the setpoint tracing of the NH_3 control is improved by using LQR. The cascade control with these control systems improves the performance of the SCR control. A multirate time sampling and an order reduction of the controller prevent a large computation load.

In order to verify the practical usability experimental tests have been carried not only the design condition but

* Toshiba Corporation
** Tokyo Electric Power Company

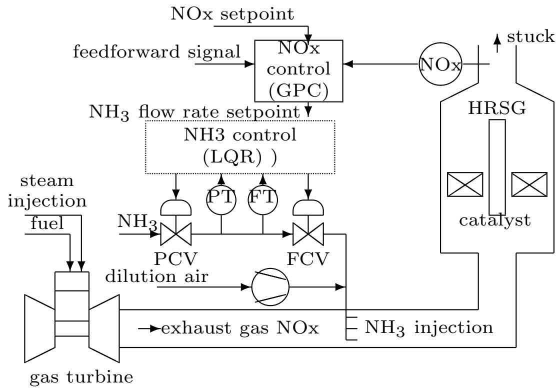

Fig. 1 NO_x reduction process

also fully normal operational conditions which include the shut down operation and the start up operation.

Since the NH_3 control is already described in the paper [7], this paper describes mainly the overall configuration of the SCR control and the NO_x control.

In the following section, the objects of the SCR control are explained. The plant model and the control design are described in section 3 and section 4. Section 5 shows the test results and the last section is the conclusion.

2. Process description

2.1 NOx reduction system

Figure 1 shows a schematic diagram of a test plant that consists of a gas turbine (GT) and an SCR in a heat recovery steam generator (HRSG).

NO_x is produced by combustion in a GT combustor and is decomposed to nitrogen (N_2) and water (H_2O) by NH_3 at the catalyst in the HRSG. The NOx gas from the gas turbine is mainly composed of nitrogen mono oxide (NO) and is decomposed by NH_3 according to

$4NO+4NH_3+O_2 \rightarrow 4N_2+6H_2O$.

The NO_x flow rate to an environment is obtained by a product of a GT exhaust gas flow rate and a concentration of NO_x which is measured at the stuck of the HRSG. The NH_3 flow rate and pressure are modulated by two control valves.

Steam injection (SI) is supplied to the combustor of the GT and can change a NOx production rate. The SI flow rate varies in accordance with the GT operation and is not dependent on the SCR control. In a particular test case, SI is adjusted manually in order to make a test condition.

2.2 Purposes of the SCR control

The purpose of the SCR control is to maintain the NO_x emission flow rate to the setpoint by modulating the NH_3 flow rate. The SCR control system has a cascade scheme that consists of NOx control and NH_3 control. The NO_x control sets an NH_3 flow setpoint in order to keep the NO_x emission flow rate to the NO_x setpoint. The NH_3 control adjusts the NH_3 flow rate to the setpoint given by the NO_x control, and retains the NH_3 pressure within allowable range.

2.3 NH_3 control

The NH_3 pressure and the flow rate are controlled by two valves, connected serially on a pipe. The features of the NH_3 control are summarized as follows:

(1) There is an interaction between two control objects.

(2) The response time of the NH_3 control is about one-tenths of the response time of the NO_x control.

2.4 NO_x control

The features of the NO_x control are summarized as follows:

(1) The NO_x emission flow rate is the product of the GT exhaust gas flow rate and the NO_x concentration. The measured signal of the NO_x concentration has a dead time which is caused by the transportation of the samplled gas and is about 2.5 minutes.

(2) The NO_x emission flow rate frequently changes according to the gas turbine operation, which includes a slow and large load change such as a start up or a shut down operation and a rapid and small load change in order to regulate a power system frequency. The NO_x emission flow rate also can be changed by the SI operation by about 20% and 1%/sec.

(3) NO_x flow from the gas turbine is the dominant disturbance. The NO_x flow rate generated by the gas turbine is estimated by the gas turbine condition. Therefore, this estimate is used for a feedforward signal. There is about 10% discrepancy in this estimate.

(4) NH_3 flow also has a transportation delay about 10 second.

2.5 Conventional control

A diagram of a conventional control is shown in **Fig. 2**. This control system has a cascade scheme which includes a NO_x control and a NH_3 control. The NO_x control makes a NH_3 flow rate setpoint, which is a summation of an integrator signal, an estimate of the NO_x generation rate, and a signal made by a plant output demand. The NH_3 flow control and the NH_3 pressure control are independent PI controllers.

3. Plant model for a control design

It is difficult to make a theoretical model of the test plant for a control design becouse there are many undefined model parameters. A plant model for the NH_3 pro-

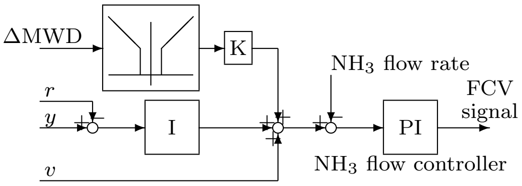

Fig. 2 Conventional control block diagram

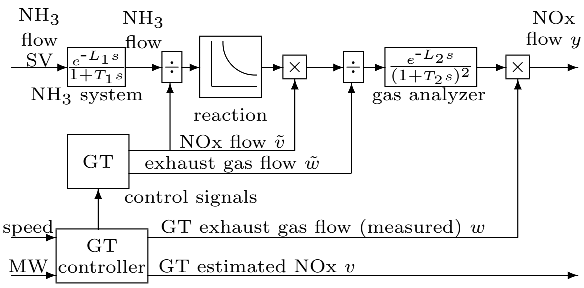

Fig. 3 NO_x plant model (nonlinear model)

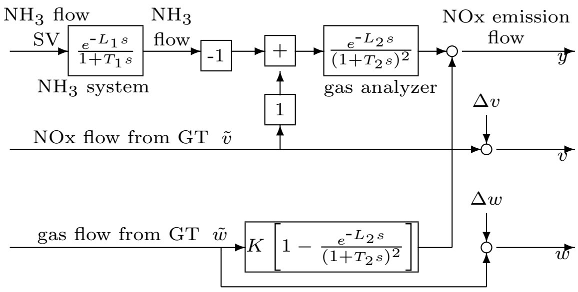

Fig. 4 NO_x plant model (linearlized model)

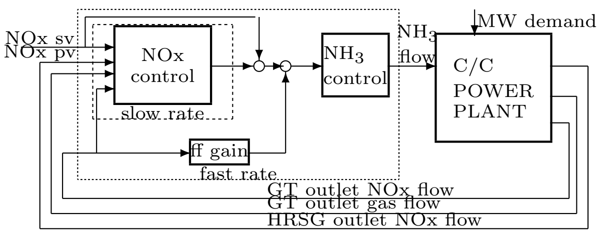

Fig. 5 Configuration of the SCR contorller

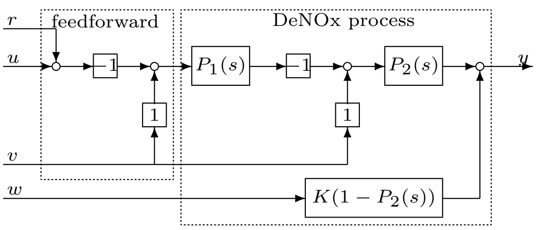

Fig. 6 GPC design model

cess is obtained [7] by a system identification with the M-sequence signal [1]. On the other hand, it is hard to make a plant model for the NO_x process by the system identification test becouse there are restrictions of the test condition and effects of disturbances. Therefore, the model structure of the NO_x process is determined by physical considerations, and the parameters in this model are obtained from step response tests.

Figure 3 shows a schematic diagram of the nonlinear NO_x process model. In this model, the NH_3 process is approximated by the first order delay and the dead time. At the catalyst, the outlet NO_x flow rate is a product of the inlet NO_x flow rate and a reaction ratio which is determined by the NH_3 flow rate and the NO_x flow rate. The concentration of NO_x at the outlet of the HRSG is a division of the NO_x flow rate by the GT exhaust gas flow rate $\tilde{w}$. A dynamics of the NO_x measurement system is modeled by the second order delay and a dead time. The measurement signal of the NO_x emission flow y is the product of the NO_x concentration and the measured GT gas flow w. A linearized model for the control design is shown in **Fig. 4**.

4. Configuration of a control system

4.1 Cascade and disturbance feedforward scheme

Figure 5 shows the proposed SCR control system which has a cascade and multirate scheme of the NH_3 control and the NO_x control. The NH_3 control receivs the NH_3 flow rate demand from the NO_x control. NH_3 pressure is regulated at the constant setpoint. The NO_x control consists of the feedback control of the NO_x emission flow rate y, and the feedforward control with the estimate of the NO_x generation rate v.

There are several reasons of this control scheme:

(1) The NH_3 control can be operated solely.

(2) The suitable design methods can be applied to the each control object.

(3) A multirate control arrangement is suited for the SCR control because the response time of the NH_3 process and the NO_x process is largely different.

(a) The NH_3 control works at the fast sampling rate.

(b) The NO_x feedback control works at the slow sampling rate.

(c) The feedforward control by using the estimate of the NO_x production rate works at the fast sampling rate in order to reject effects of the change of the NO_x production rate.

(4) A deviation of the NH_3 process becomes smaller by the feedback control.

4.2 NH_3 control

The NH_3 process is an interactive multivariable system that has two inputs and two outputs. An LQR method is applied to design a NH_3 controller. The design method is briefly described. The plant is represented by the state space model

$$x_{k+1} = Ax_k + Bu_k \quad (1)$$

$$y_k = Cx_k \quad (2)$$

where $A \in R^{n\times n}$, $B \in R^{n\times m}$, $C \in R^{r\times n}$. The controller to be designed should have the following functions:

- servo type controller in order to avoid an offset.
- observer to estimate the state variable.

The controller is represented by the equations

$$\hat{x}_{k+1} = A\hat{x}_k + Bu_k + L(y_k - \hat{y}_k) \quad (3)$$

$$w_{k+1} = w_k + (r_k - y_k) \quad (4)$$

$$\hat{u}_k = F_1\hat{x}_k + F_2 w_k \quad (5)$$

$$u_k = u_{min} < \hat{u}_k < u_{max} \quad (6)$$

where $\hat{x}_k$, w_k, r_k are the state vector of the observer, the state vector of the integrator and the setpoint vector. The feedback gain F_1 and F_2 are given by solving the Riccati equation

$$\begin{aligned} P &= A_c^T P A_c + Q \\ &\quad - A_c^T P B_c (R + B_c^T P B_c)^{-1} B_c^T P A_c \quad (7) \\ F &= -(R + B_c^T P B_c)^{-1} B_c^T P A_c \quad (8) \end{aligned}$$

where,

$$A_c = \begin{bmatrix} A & 0 \\ -C & I \end{bmatrix}, B_c = \begin{bmatrix} B \\ 0 \end{bmatrix}$$

$$Q = \begin{bmatrix} C^T Q_1 C & 0 \\ 0 & Q_2 \end{bmatrix}, F = [F_1 \ F_2]$$

in which Q_1, Q_2, R are a weighting matrix for the plant outputs, a weighting matrix for the states of integrator and a weighting matrix for the manipulated values. The observer gain L is chosen such that $A - LC$ is stable. The order of the controller is reduced by an order reduction method [9].

In order to simplify the NH_3 controller, the controller designed at a rated condition uses for all other plant condition.

4.3 NO_x control

The NO_x control system includes the feedforward signal of the NO_x flow rate generated by the gas turbine and the feedback compensator designed using GPC. In order to prevent the unpreferable response, the feedback compensator is made by the two degree of freedom configuration.

4.3.1 Design model of the NO_x control

Figure 6 shows a design model of the NO_x control, where r is a reference of the NO_x flow rate, u is a manipulated value made by the GPC, v is an estimates of the NO_x flow rate generated by the gas turbine, w is an exhaust gas flow rate and y is a NO_x emission flow rate, $P_1(s)$ is a transfer function of the NH_3 flow process, and $P_2(s)$ is a transfer function of the NO_x measurement system. The design model for the NO_x control is described by

$$\begin{aligned} y &= P_2(v - P_1(v - (u + r))) + K(1 - P_2)w \\ &= P_1P_2(u + r) - P_2(P_1 - 1)v + K(1 - P_2)w. \quad (9) \end{aligned}$$

4.3.2 Prediction model

In order to take account of the feedforward control, the prediction model includes the disturbance signal w and v and the reference signal r. Descritizing (9), the equation of the prediction model is described by

$$\begin{aligned} Ay(t) &= B_1(r(t-1) + u(t-1)) + B_2w(t-1) \\ &\quad + B_3v(t-1) \quad (10) \end{aligned}$$

where, A, B_1, B_2, B_3 are polynomials of z^{-1}. The j step ahead prediction model is

$$\begin{aligned} \hat{y}(t+j) &= G_j\Delta u(t+j-1) + F_jy(t) + H_j\Delta u(t-1) \\ &\quad + K_j\Delta w(t+j-1) + L_j\Delta w(t-1) \\ &\quad + M_j\Delta v(t+j-1) + N_j\Delta v(t-1) \\ &\quad + G_j\Delta r(t+j-1) + H_j\Delta r(t-1) \quad (11) \end{aligned}$$

where $\hat{y}(t+j)$ is a j step ahead prediction of $y(t)$, $\Delta = 1 - z^{-1}$, and $F_j, G_j, H_j, K_j, L_j, M_j, N_j$ are polynomials of z^{-1} which satisfy the following Diophantine equations

$$\begin{aligned} 1 &= E_jA\Delta + z^{-j}F_j, \quad E_jB_1 = G_j + z^{-j}H_j \\ E_jB_2 &= K_j + z^{-j}L_j, \quad E_jB_3 = M_j + z^{-j}N_j. \end{aligned}$$

4.3.3 Calculation of controller gains

The performance index J is defined as

$$\begin{aligned} J &= \sum_{j=1}^{N_P}\{(\hat{y}(t+j) - r(t+j))^2 \\ &\quad + \lambda\Delta u(t+j-1)^2\} \quad (12) \end{aligned}$$

where N_P is an interval to be observed and λ is a weighting variable. The manipulated variables $\Delta u(t+j-1), j = 1, \ldots, N_P$ which minimize the performance index make $\partial J/\partial\Delta\hat{u} = 0$ [3] and are given as

$$\begin{aligned} \Delta\hat{\boldsymbol{u}} &= -(\lambda I + G^TG)^{-1}G^T(F\boldsymbol{y} + H\Delta\boldsymbol{u} + K\Delta\hat{\boldsymbol{w}} \\ &\quad + L\Delta\boldsymbol{w} + M\Delta\hat{\boldsymbol{v}} + N\Delta\boldsymbol{v} + G\Delta\hat{\boldsymbol{r}} + H\Delta\boldsymbol{r} - \hat{\boldsymbol{r}}) \quad (13) \end{aligned}$$

where $\boldsymbol{y} = [y(t)\cdots y(t-n)]^T$, $\hat{\boldsymbol{r}} = [r(t+1)\cdots r(t+N_P)]^T$,

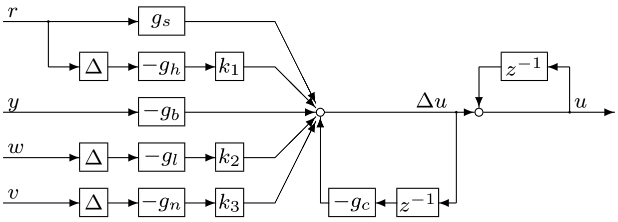

Fig. 7 GPC controller

$\boldsymbol{r} = [r(t-1)\cdots r(t-m)]^T$, $\hat{\boldsymbol{u}} = [u(t)\cdots u(t+N_P-1)]^T$, $\boldsymbol{u} = [u(t-1)\cdots u(t-m)]^T$, $\hat{\boldsymbol{w}} = [w(t)\cdots w(t+N_P-1)]^T$, $\boldsymbol{w} = [w(t-1)\cdots w(t-l)]^T$, $\hat{\boldsymbol{v}} = [v(t)\cdots v(t+N_P-1)]^T$, $\boldsymbol{v} = [v(t-1)\cdots v(t-q)]^T$, n, m, l, q are the orders of $A(z^{-1})$, $B_1(z^{-1})$, $B_2(z^{-1})$, $B_3(z^{-1})$, G, K, M are $N_P \times N_P$ lower triangular matrices which $(i,\ k)$ elements are the $z^{-(i-k)}$th coefficients of the polynomials G_j, K_j, M_j, F, H, L, N are $N_P \times (n+1)$, $N_P \times m$, $N_P \times l$, $N_P \times q$ matrices which $(j,\ k)$ elements are the $z^{-(i-k)}$th coefficients of the polynomials G_j, K_j, M_j, N_j.

The first element $\Delta u(t)$ of $\Delta\hat{\boldsymbol{u}}$ is used for the manipulated value at time t. In the equation (13) there are future disturbances $\hat{\boldsymbol{v}}, \hat{\boldsymbol{w}}$ which can not be available because these value are not predictable. $\Delta u(t)$ is written by the available variables $\boldsymbol{r}, \boldsymbol{y}, \boldsymbol{w}, \boldsymbol{v}$.

$$\begin{aligned}\Delta u(t) &= g_s r(t) - g_b(z^{-1})y(t) - g_c(z^{-1})\Delta u(t-1) \\ &\quad - g_n(z^{-1})\Delta v(t) - g_l(z^{-1})\Delta w(t) \\ &\quad - g_h(z^{-1})\Delta r(t) \qquad (14)\end{aligned}$$

where, $g_s = g\,[1\cdots 1]^T$, $g = [1\ 0\cdots 0](\lambda I + G^T G)^{-1}G^T$, g_b, g_c, g_n, g_l, g_h are polynomials of z^{-1} and their coefficients are $[g_{b,0}\cdots g_{b,n}] = gF$, $[g_{c,0}\cdots g_{c,m-1}] = gH$, $g_{n,0} = gM\,[1\,0\cdots\ 0]^T$, $[g_{n,1}\cdots g_{n,r}] = gN$, $g_{l,0} = gK\,[1\,0\cdots\ 0]^T$, $[g_{l,1}\cdots g_{l,l}] = gL$, $g_{h,0} = gG\,[1\,0\cdots\ 0]^T$, $[g_{h,1}\cdots g_{h,m}] = gH$.

4.3.4 NO_x controller by GPC

A schematic diagram of the NO_x controller is shown in **Fig. 7**., where k_1, k_2, k_3 are weighting values of disturbances and reference signal. Since these signal do not effect the closed loop properties, weighting values can independently be adjusted.

5. Test results

Experimental results are given that demonstrate the improved performance achieved by the control method described in the previous section. The tests were accomplished in not only the design condition but also a condtion in which a plant load changes largely.

The unit of x-axis of the following graphs is time (second) and the unit of y-axis is a normalized process value.

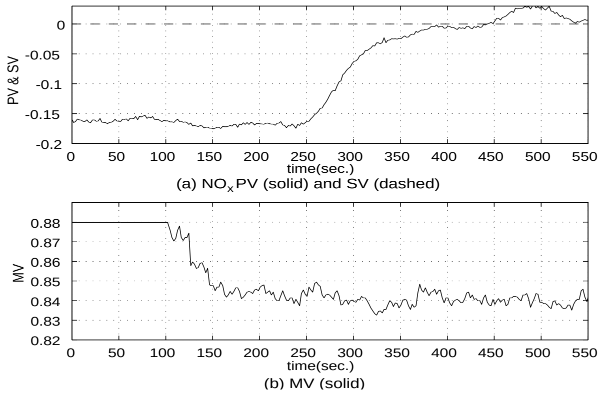

Fig. 8 Feedback control

5.1 Control parameters

The sampling rate of the NH_3 control and the feedforward control is 0.2 second. The sampling rate of the GPC is 5 second or 20 second which is selected and compared to verify control performances. The design parameters for the GPC design were decided by tuning tests and classified according to the sampling rate of the GPC:

5 sec. $P_1 = e^{-10s}/(1+10s)$, $P_2 = e^{-110s}/(1+15s)^2$ $N_P = 40$, $\lambda = 20$

20 sec. $P_1 = e^{-20s}$, $P_2 = e^{-100s}/(1+30s)$ $N_P = 10$, $\lambda = 2$

The dead time of P_2 is the dominant factor of the plant dynamics which is the delay of the measurement and a constant in almost all conditions.

5.2 Feedback performance of the GPC

Figure 8 shows the test results which present a feedback performance of the GPC with sampling rate 20 second. In this test, the controller is initially manual and changed to auto-mode at 100 second. In Fig. 8(a), a solid line shows the process output y (PV) which is the NO_x emission flow rate and a dashed line shows the set point r (SV). The output of the GPC u (MV) is shown in Fig. 8(b). When the GPC becomes auto-mode, the MV value changes within 100 seconds and do not change significantly after that. On the other hand, the process output y do not move for 150 seconds which is accordance with the process dead time, and reach the set point within 100 seconds. This motion is different from a motion of a PI controller that will change MV continuously whenever there is a error between y and r. Thus, this figure shows an fulfillment the GPC design which compensates a dead time.

5.3 Various Design of GPC

In this section the GPC design presented in this paper is compared with a conventional control and the GPC design in the paper [11].

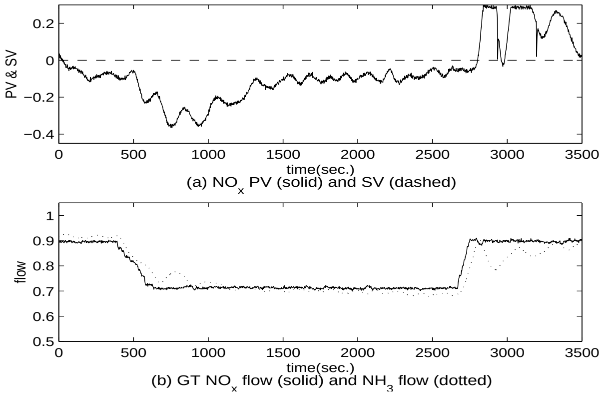

Fig. 9 SI flow change – conventional control

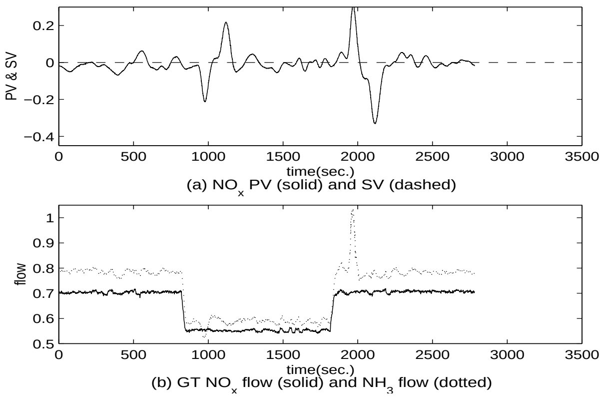

Fig. 10 SI flow change – GPC + LQR

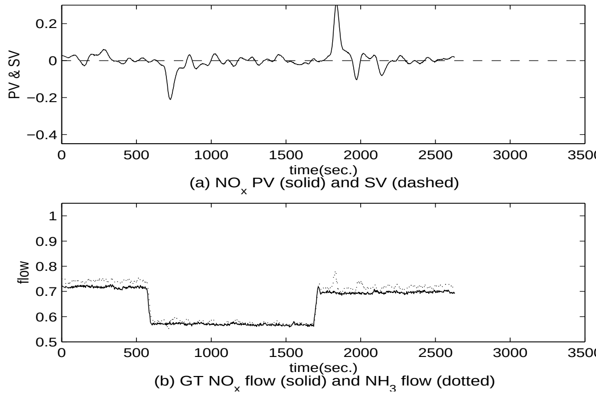

Fig. 11 SI flow change – GPC(design with FF model) + LQR

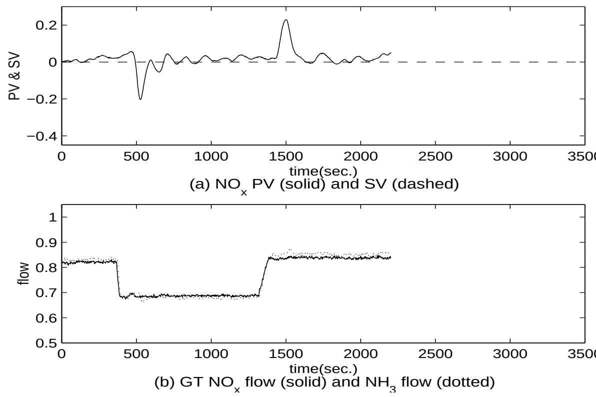

Fig. 12 SI flow change – GPC (20sec) + LQR

In order to make a test condition, the NO$_x$ production rate is changed by the SI operation. Since this test does not change the plant condition exclude the NO$_x$ flow rate, it is clear to evaluate a performance of a controller.

Figures 9–12 show the test results of the conventional control, the standard GPC design [11], the presented GPC design (sampling 5 sec.), and the presented GPC design (sampling 20 sec.). In graph (a) of each figure, a solid line shows the process output y (PV) and a dashed line shows the set point r (SV). In graph (b), a solid line shows the estimate of the NO$_x$ production rate v and a dashed line shows the NH$_3$ flow rate. A histogram for an error between y and r is shown in **Fig. 13**, and a mean of absolute values and a mean of squared values of the errors are shown in **Table 1**.

The proposed method reduces the average values of the errors by one third to one fifth of the average values of conventional method.

When a NO$_x$ production rate changes, at the beginning the output y changes to same direction by this disturbnace. The standard GPC design has a large undershoot after that as shown in Fig. 10. Figures 11, 12 show that the proposed method prevents this unpreferable action.

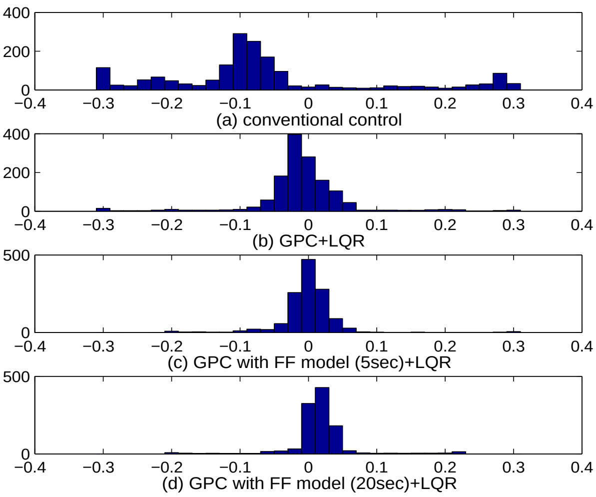

Fig. 13 Distribution NO$_x$ PV at SI flow change

Table 1 SI flow change test

type	$\frac{1}{N}\sum\lvert e\rvert$	$\frac{1}{N}\sum e^2$
conventional control	0.14046	0.02809
GPC(5sec) + LQR	0.04197	0.005163
GPC with FF model(5sec) + LQR	0.02682	0.002465
GPC with FF model(20sec)+ LQR	0.03067	0.002591

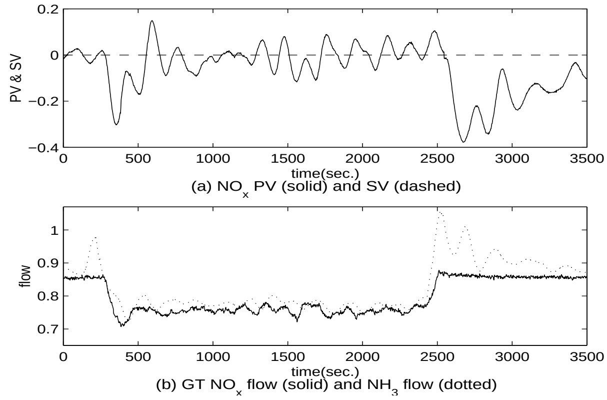

Fig. 14 Conventional control

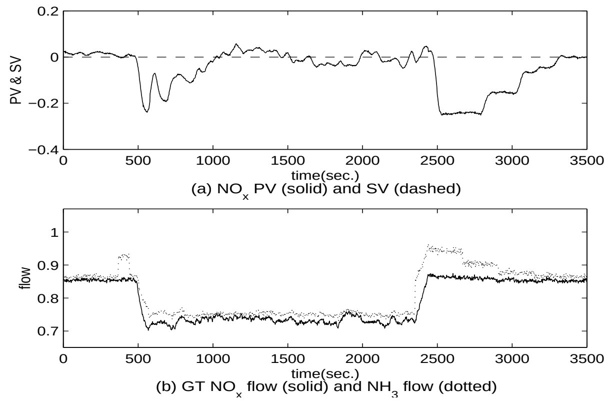

Fig. 15 NO$_x$ - conventional, NH$_3$ - LQR

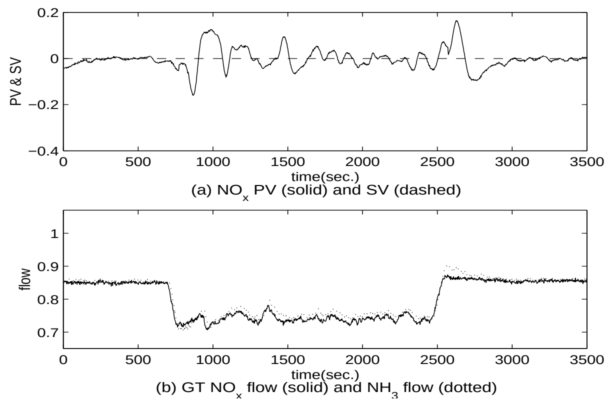

Fig. 16 NO$_x$ - GPC, NH$_3$ - PI

5.4 Combination of control algorithms

In order to evaluate which of the controllers is dominant to improve a performance, various combination of control methods are tested. The combination of the NO$_x$ and NH$_3$ control and test results are as follows:

- conventional control + PI (in **Fig. 14**)
- conventional control + LQR (in **Fig. 15**)
- GPC + PI (in **Fig. 16**)
- GPC + LQR (in **Fig. 17**)

The test condition is a 5% plant load change. In graph (a) of each figure, a solid line shows the process output y (PV) and a dashed line shows the set point r (SV).

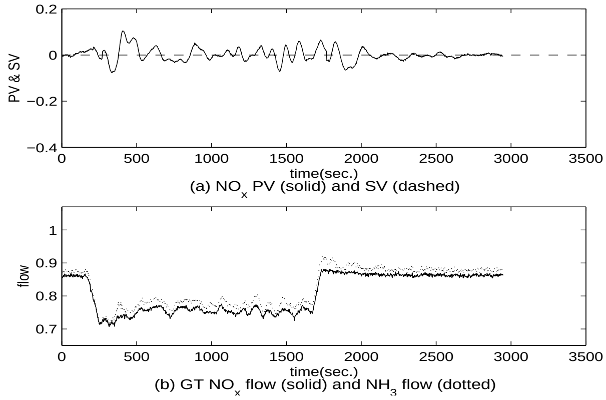

Fig. 17 GPC + LQR

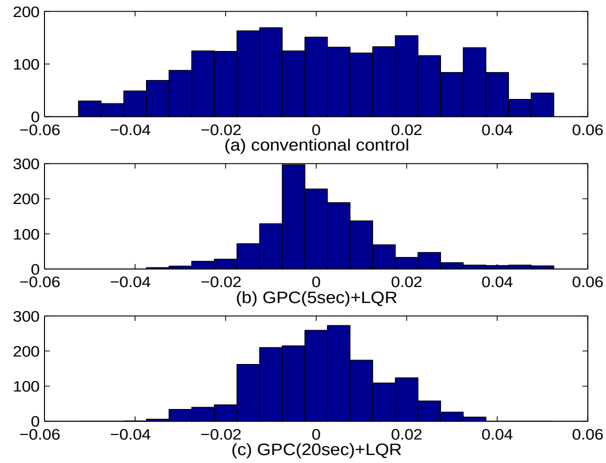

Fig. 18 Distribution NO$_x$ PV at steady condition

Table 2 Steady condition

type	$\frac{1}{N}\sum\lvert e\rvert$	$\frac{1}{N}\sum e^2$
conventional control	0.02065	6.065×10^{-4}
GPC (5sec) + LQR	0.009711	1.777×10^{-4}
GPC (20sec)+ LQR	0.01067	1.777×10^{-4}

In graph (b), a solid line shows the estimate of the NO$_x$ production rate v and a dashed line shows the NH$_3$ flow rate.

The response of **Fig.** 14 and **Fig.** 15 in which the NO$_x$ controller is the conventional control is a similar. The response of **Fig.** 16 and **Fig.** 17 in which the NO$_x$ controller is the GPC is a similar. In the case that the NH$_3$ controller is PI control, fluctuations of the NH$_3$ flow rate affect the NO$_x$ emission flow rate. The LQR regulate the NH$_3$ steadily and fluctuations of the NO$_x$ flow rate are much smaller than the case of PI control.

5.5 Control performance : constant load

This test evaluates a performance of the conventional control and the proposed control at a constant load demand. Although the plant load demand is constant, a gas turbine changes a combustion rate by a frequency fluctuation of a power system and the NO$_x$ production rate changes at random. A histogram for an error between y

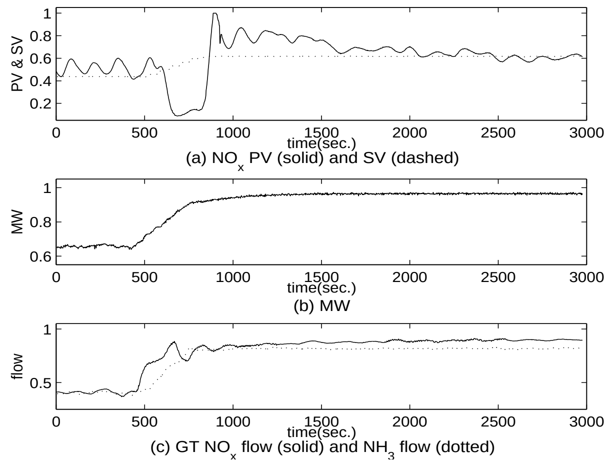

Fig. 19 Load change - conventional control

and r is shown in **Fig. 18**, and a mean of absolute values and a mean of squared values of the errors is shown in **Table 2**. The mean value of the error by the proposed method is smaller than the conventional control by one half or one third.

5.6 Control performance : load change

Figures 19–21 show the test results of the conventional control and the proposed control in the case of a load demand change. In graph (a) of each figure, a solid line shows the process output y (PV) and a dashed line shows the set point r (SV). In graph (b), a solid line shows the estimate of the NO_x production rate v and a dashed line shows the NH_3 flow rate.

A histogram for an error between y and r is shown in **Fig. 22**, and a mean of absolute values and a mean of squared values of the errors is shown in **Table 3**. The mean value of the error by the proposed method is smaller than the conventional control by one third or one tenth.

5.7 Control performance : startup

This test evaluates a performance of the controllers during a plant start up. The SCR control does not work until prescribed conditions are satisfied. After the conditions are satisfied, the SCR control works automatically. Since the proess parameters change largely, the stability of the controller is important.

Figures 23–25 show the test results of the conventional control and the proposed control in the case of a load demand change. In graph (a) of each figure, a solid line shows the process output y (PV) and a dashed line shows the set point r (SV). In graph (b), a solid line shows the electric output (MW) and a dashed line is a fuel flow rate of the gas turbine. In graph (c), a solid line shows the NO_x production rate v and a dashed line shows the NH_3 flow rate.

In each test, the SCR controller becomes automatic

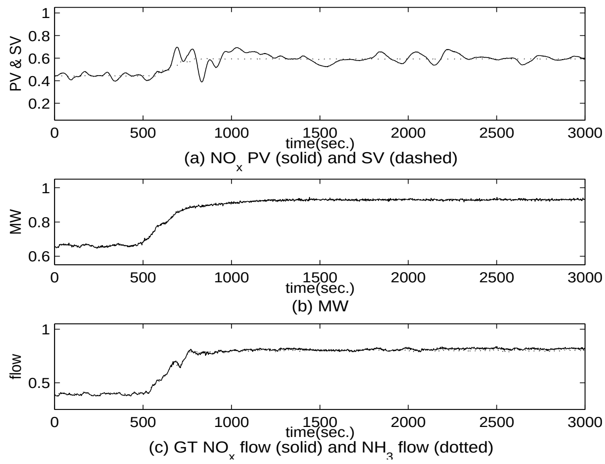

Fig. 20 Load change - GPC(5sec)+LQR

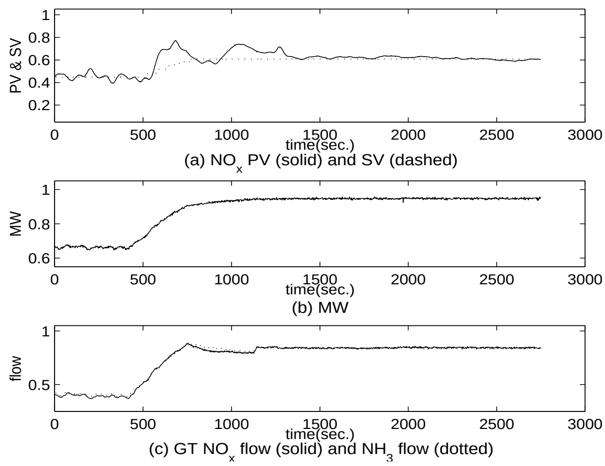

Fig. 21 Load change - GPC(20sec)+LQR

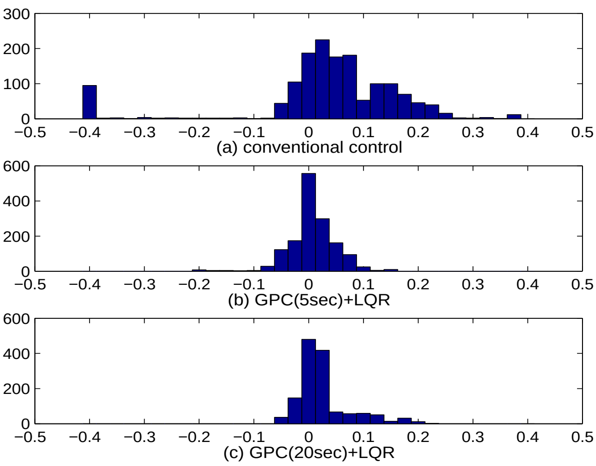

Fig. 22 Load change - disutribution of NO_x deviation

Table 3 Load change test

type	$\frac{1}{N}\sum\|e\|$	$\frac{1}{N}\sum e^2$
conventional control	0.1050	0.02417
GPC (5sec) + LQR	0.03003	0.001867
GPC (20sec)+ LQR	0.03405	0.003010

mode between 1200 second and 1300 second and starts an injection of NH_3. Since the gas turbine has already started and produced NO_x, a large amount of the NO_x emission continues until 1300 second or 1500 second. The SI starts at around 2000 second and the NO_x production rate decreases extremely. The NO_x production rate increases again along with the gas turbine loading up. The plant reaches at the rated load at around 3000 second.

A histogram for an error between y and r is shown in **Fig. 26**, and a mean of absolute values and a mean of squared values of the errors is shown in **Table 4**. The mean value of the error by the proposed method is smaller than the conventional control by one half.

The controller that has a constant parameter can work stably in this test. The reasons are as follows:

- As stated in the section 5.1, the dead time of the measurement system, which is the dominant factor for a control, is constant.
- The reaction of NO_x and NH_3 at the catalyst is linear as shown in **Fig. 27**, where the x axis is the ratio of the NH_3 flow rate to the NO_x flow rate and the y axis is the ratio of the unreacted NO_x flow rate to the NO_x flow rate.

5.8 Summary of test results

The following features are evaluated by the experimental tests:

- the feedback performance is improved
- the performance by the combination of the GPC and the LQR is superior to others
- the proposed GPC design prevents the undershoot at the disturbance change
- the error by using the proposed control is less than one half of the error by the conventional control
- the constant control parameter can be used in full operation range
- the performance for the disturbance rejection by using GPC with a short sampling rate is better than by using GPC with a long sampling rate

6. Conclusion

An SCR control system which consists of an LQR and a GPC incorporated with a feedforward control has been developed. The control system has a cascade and a multi-rate sampling scheme that includes NO_x control designed by the GPC method and NH_3 contorol designed by the LQR method.

The SCR controller has been verified by experimental tests which carried out not only in a design condition but also in various condition on a utility power plant.

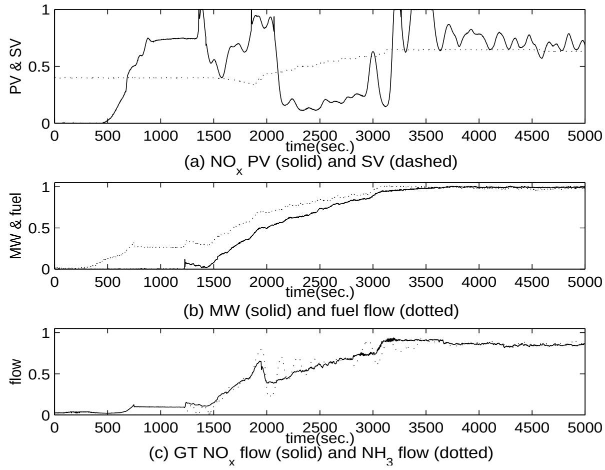

Fig. 23 Start up - conventional control

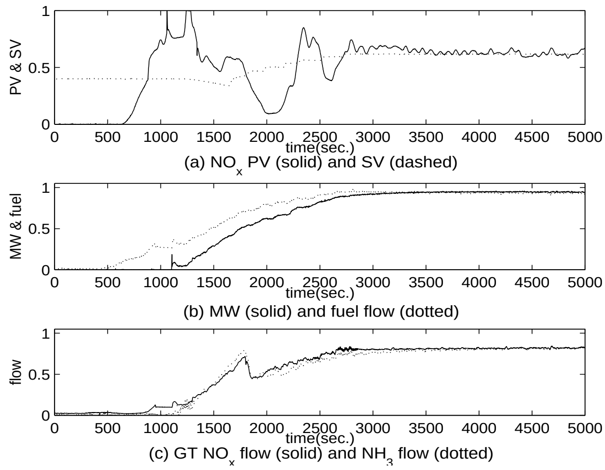

Fig. 24 Start up - GPC(5sec)+LQR

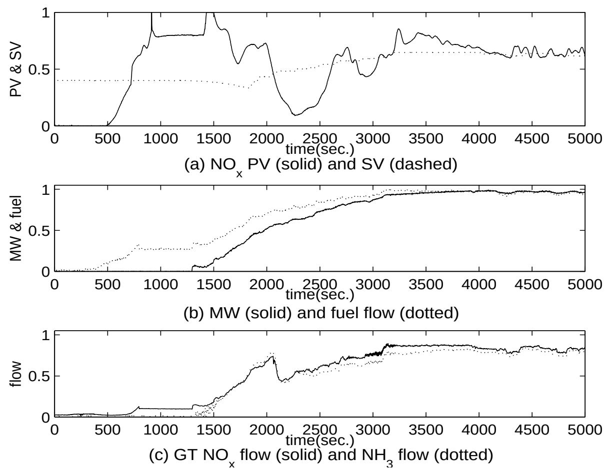

Fig. 25 Start up - GPC(20sec)+LQR

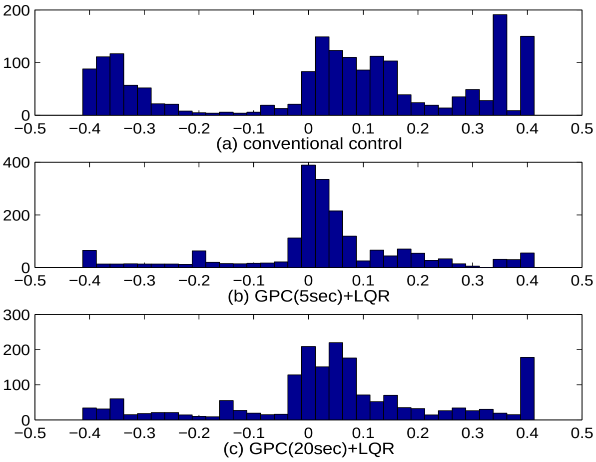

Fig. 26 Start up - distribution of NO_x deviation

Table 4 Start up

type	$\frac{1}{N}\sum\lvert e\rvert$	$\frac{1}{N}\sum e^2$
conventional control	0.2283	0.07695
GPC (5sec) + LQR	0.1132	0.03055
GPC (20sec)+ LQR	0.1582	0.04951

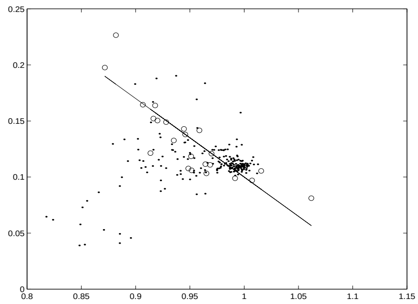

Fig. 27 NO_x reaction

This paper shows that the SCR control has been designed systematically by using the multiple design methods which are suitable to different control objects and also this control system has improved the performance.

References

1) S. Adachi : Theory of System Idendtification for Users (in Janpnese), SICE (1993)
2) B. D. O. Anderson and J. B. Moore : Linear Quadratic Optimal Control, Prentice-Hall (1990)
3) R. R. Bitmead, M. Gevers and V. Wertz : Adaptive Optimal Control - The Thinking Man's GPC, Prentice-Hall (1991)
4) T. Hirasawa, M. Akiyama, T. Ohki, T. Inoue and T. Hara : The Application of Fuzzy Control on Boiler Flue Gas NOx Removal Reactor, Proceedings-D of ASME the 71st Mechanical Engineering Congress, 488/490 (1993)
5) T. Nagai, K. Sagara, H. Takatsuka and M. Demoto : Improvement of NH_3 Injection Control System for a Selective Catalyst NOx Removal System (in Japanese), Mitsubisi Heavy Industries Technical Review, 25-1, 32/36 (1988)
6) M. Nakamoto, T. Kokubo, K. Shimizu and J. Funaki : Two-Degree of Freedom Configuration of Generalized Predictive Control to Increase the Ability of the Disturbance Rejection and the Setpoint Tracking for a Dead Time System (in Japanese), Transactions of ISCIE, 10-6, 297/303 (1997)
7) M. Nakamoto, T. Kokubo, A. Nakai and H. Tanabe : Application of Linear Quadratic Regulator to an Interactive Flow Control System for a Thermal Power Plant (in Japanese), Transactions of SICE, 33-6, 494/501 (1997)
8) JSME : JSME Mechnical Engineers' Handbook Applications (in Japanese), Maruzen (1987)
9) G. Obinata : Order Reduction of a Control System Using Balanced Realization, Hankel Norm and Continued Fraction (in Japanese), Journal of ISCIE, 34-9, 508/514 (1990)
10) D. E. Seborg, T. F. Edgar and D. A. Mellichamp : Process Dynamics and Control, John Wiley & Sons (1989)
11) K. Shimizu, M. Nakamoto, T. Kokubo and H. Tanabe : Generalized Predictive Control for a NOx Decomposition Process (in Japanese), Transactions of SICE, 32-6, 912/920 (1996)
12) K. Ucida, M. Nakamoto, Y. Chida, H. Ezure, H. Imanari, R. Watanabe, T. Kida and T. Hirata : Practical Application of H_∞ Control (in Japanese), SICE (1996)
13) I. Yokoyama, M. Kawakami, T. Ito and Y. Kato : NOx Reduction Control using the Fuzzy Control Logic for a Coal Fired Thermal Power Plant (in Japanese), Denki Hyoron, 1994-3, 46/51 (1994)

Masashi Nakamoto
received the M.E. and Dr. Eng. degree from Osaka University, in 1979 and 1997, respectively. From 1979, he has been working in Toshiba Corporation.

Takashi Kokubo
received the M.E. degree from Seikei University in 1980. From 1980, he has been working in Tokyo Electric Power Company.

Akinori Kamito
received the M.E. degree from Hokkaido University in 1994. From 1994, he has been working in Toshiba Corporation.

Keiko Shimizu
received the B.S. degree from Tohoku University in 1988, and Dr. Eng. degree from Kyoto University in 2001. From 1988, she has been working in Toshiba Corporation.

Reprinted from Trans. of the SICE
Vol. 36 No. 11 962/971 2000